



Inhibition of Low Carbon Steel Pipes of Heat Exchangers in Industrial Water Medium by Some Plants Extract

A. M. Badiea^{1,*}, Hani A. Dammag², A. S. Abdulghani¹, Kikkeri N. Mohana³

¹Department of Industrial and Manufacturing System Engineering, Engineering College, University of Taiz, Habel Salman, Taiz, Yemen

²Department of Chemical Engineering, Engineering and Petroleum College, University of Hadhramout of Science and Technology, Mukalla, Hadhramout, Yemen

³Department of Studies in Chemistry, University of Mysore, Manasagangotri, Mysore- 570 006, India

Received 15 Aug 2012, Revised 25 Dec 2012, Accepted 25 Dec 2012

* Corresponding author. E-mail address: badeea7@yahoo.com (Badiea Abdullah M.), Tel.: +967 773 117 252,

Abstract

Inhibition efficiencies of *Ocimum basilicum* and *Cucurbita pepo* extracts on low carbon steel corrosion in industrial water have been investigated using mass loss, potentiodynamic polarization, impedance spectroscopy and SEM. It was found that the plant extracts chosen revealed good performance as green inhibitors for low carbon steel in industrial water, and their inhibitive performance improved with increasing concentration up to critical values of 2.96 and 5.25 g L⁻¹ for *Cucurbita* and *Ocimum*, respectively. Thermodynamic parameters were evaluated and discussed. SEM was carried out to characterize the film formed on the metal surface.

Keywords: Low Alloy Steel, SEM, Polarization, Corrosion, Mass Loss

Introduction

Low carbon steel is used considerably in the manufacture of pipelines for many industries, particularly for use in the petroleum industries. Corrosion problems occur in these pipelines due to the aggressive environment of fluid through them, whether oil or water. In heat exchangers, all types of water used for cooling down or heating up the products contain very high chloride concentrations and other anions of metals and bicarbonates. Failure of pipes or valves might lead to stop or shutdown of surface facilities. Therefore, injection of corrosion inhibitors through different sites of pipes to protect the facilities from failure is very important. The inhibition of mild steel corrosion in aqueous solution by organic [1-3] and inorganic [4, 5] compounds has been studied extensively. Most of the efficient inhibitors used in industries are organic compounds having multiple bonds in their molecules [6], which contain nitrogen and sulfur atoms that are adsorbed on the metal surface. These inhibitors may cause reversible (temporary) or irreversible (permanent) damage to organ systems viz., kidneys or liver, or may disturb a biochemical process or to disturb an enzyme system at some site in the body [7]. The toxicity may manifest either during the synthesis of the compound or during its application. These toxic effects have led to the use of natural products as anticorrosion agents which are eco-friendly and harmless. The increasing pollution levels in today's world make it necessary to predict the necessity in the future of controlling the corrosion process that was formerly left by the action of nature. Further, the known hazardous effects of most synthetic corrosion inhibitors are the motivation for the use of some natural products. Recently, plant extracts have again become important as an environmentally acceptable, readily available and renewable source for a wide range of needed inhibitors. Plant extracts are viewed as an incredibly rich source of naturally synthesized chemical compounds that can be extracted by simple procedures with low cost. However,

synergistic and antagonistic effects are often expected with these mixtures of inhibitors that may affect their inhibition efficiency.

It is well known that the application of plant extracts is one solution among practical methods for protection of metals against atmospheric corrosion because it is clean, environment-friendly and readily available. A number of natural compounds [8-18] have been reported as corrosion inhibitors for metals and their alloys in acidic, alkaline and neutral solutions. In the present investigation, a study has been done to use *Ocimum basilicum* L (Sweet Basil) and *Cucurbita pepo* L (Pumpkin), as corrosion inhibitors for low carbon steel in industrial water as a cheap and friendly corrosion inhibitor. *Cucurbita pepo* raw or cooked is edible and can be used for medicines [19]. Likewise, *Ocimum basilicum* is edible and an essential oil obtained from plants is used as a food flavoring in mustards, sauces, vinegars, etc. [20,21]. Thus, they are non-toxic, green and eco-friendly compounds. The components of plant extracts are transported with steam and well distributed by proper velocity to prevent steel corrosion in condenser tubes by adsorption on the metal surface or by shifting the surface pH value towards less acidic. The selection of suitable inhibitors mainly depends on the type of industrial environment, type of ions it contains, velocity of the fluid and environment temperature.

Thermodynamic parameters were obtained from electrochemical polarization measurements of the inhibition process at different temperatures. The apparent activation energy and pre-exponential factor at different concentrations of inhibitor were also calculated and their effects on the corrosion rate of low carbon steel were discussed. The rotational speeds (revolution per minute) were converted to velocities (length per time) as fluid flows through pipe using some empirical equations.

1. Experimental Work

1.1 Materials preparation

The corrosion tests were performed on low carbon steel coupons cut from pipes of heat exchangers with dimensions of 19.2 mm outside diameter, 1 mm thickness and 5 mm length (Figure 1(a) and (b)) and having the following composition (wt%): 0.15- C; 0.37- Si; 0.04- P; 0.01- Al; 0.05- Mn; 0.05- S and the remainder iron. The pH of the industrial water was 5.9 and the chemical composition (ppm) was 1.9×10^4 - Cl⁻; 950 - Ca²⁺; 650 - SO₄²⁻; 450 - Mg²⁺; 64 - HCO₃⁻; 58 - Na⁺; 7.06 - PO₄³⁻. For the gravimetric and electrochemical measurements, some treatment for the surface of specimens was carried out. Prior to each experiment, the surface of the specimen was polished under running tap water using emery paper of grade numbers, 220, 320, 450, and 600, rinsed with distilled water, dried on a clean tissue paper, immersed in benzene for five seconds, dried and immersed in acetone for five seconds and dried with clean tissue paper. Finally they were kept in a desiccator on for one hour until use.

1.2 Mass loss measurements

The initial weight of the specimen was recorded using an analytical balance (precision ± 0.1 mg) before immersion in the industrial water. The corrosion rates (v_{cor}) of low carbon steel at various immersion times (7 to 60 h), various temperatures (30 to 80°C), various concentrations (0.68 to 2.96 g L⁻¹) of *Cucurbita pepo* L and (0.90 to 5.25 g L⁻¹) of *Ocimum basilicum* L and various rotational speeds (1500 – 2100 rpm) have been determined from mass loss using Eq. (1), where W is the mass loss [g], t is the immersion time [h], and A is the outside area of the cylinder coupon [mm²]. The corrosion rate (v_{cor}) is expressed in g m⁻² d⁻¹.

$$v_{cor} = \frac{24 \times 10^6 W}{t A} \quad (1)$$

The temperature of the environment was maintained thermostatically by a controlled water bath (Weiber Comp. Ltd. India). The velocity of the specimens was set at a desired speed using speed regulator motor (Eltek Ltd.).

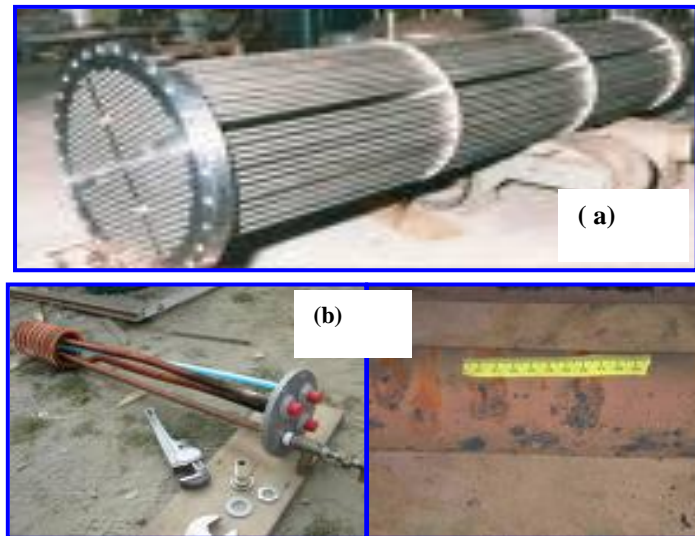


Fig. 1 Three photos of low carbon steel in heat exchanger: (a) new and (b) after working 18 months.

1.3. Electrochemical measurements and SEM

Electrochemical trends were carried out in a conventional three electrode cylindrical glass cell. The working electrode in the form of a cylinder cut from pipe steel with an outside diameter of 19.2 mm, a thickness of 1 mm and length of 5 mm, as the outside surface area, was exposed to the solution while the inside surface was embedded with epoxy resin .

A saturated calomel electrode (SCE) and platinum electrode are used as a reference and auxiliary electrode, respectively. The polarization curves were recorded with a potentiostat type EG and G 273, at a scan rate of 0.4 mV s^{-1} . The steel electrode was maintained at corrosion potential for 30 min and thereafter pre-polarized at -800 mV for 10 min. The potential was swept to anodic potentials. The test solution was aerated industrial water in the cell with and without inhibitors, which were maintained throughout the experiments. In the case of the polarization method, both cathodic and anodic polarization curves were recorded potentiodynamically using a Solartron -1480 multi-channel electrochemical interphase controlled by computer. Corrosion current density (I_{cor}) can be derived from the intersection of the cathodic and anodic Tafel slopes. Thus, the inhibition efficiency (IE) and surface coverage degree (Θ) are expressed as Eqs. (2) and (3):

$$IE_{I_{\text{cor}}} [\%] = \frac{(I_{\text{cor}})_a - (I_{\text{cor}})_p}{(I_{\text{cor}})_a} \times 100 \quad (2)$$

$$\Theta = IE/100 \quad (3)$$

where, $(I_{\text{cor}})_a$ and $(I_{\text{cor}})_p$ are the corrosion current density in absence and presence of inhibitors, respectively. Electrochemical impedance spectroscopy (EIS) was carried out with a Tacussel electrochemical system, which included a digital potentiostat model Voltalab PGZ 100 computer at E_{cor} after immersion in solution without bubbling. The outside cylinder surface of steel exposed by 302 mm^2 (i.e. 19.2 mm O.D., 1 mm thickness and 5 mm length) to the solution was used as a working electrode (WE). The inside surface of the specimen was embedded in epoxy resin, and then held in a shaft which was rotated using a $\frac{1}{4}$ hp motor-driven shaft. After the determination of steady-state current at a given potential, sine wave voltage (10 mV) peak to peak, at frequencies between 100 kHz and 10 MHz were superimposed on the rest potential. Computer programs automatically controlled the measurements performed at rest potentials after 30 min of exposure. The impedance diagrams are given in the Nyquist representation. The inhibition efficiency obtained from the charge-transfer resistance was calculated by Eq. (4).

$$IE_{EIS} \% = \frac{(1/R_{\text{ct}})_a - (1/R_{\text{ct}})_p}{(1/R_{\text{ct}})_a} \times 100 \quad (4)$$

where, $(R_{ct})_a$ and $(R_{ct})_p$ are the charge-transfer resistance values in the absence and presence of plant extracts inhibitors, respectively.

The scanning electron micrographs (SEM) of the cleaned surface of low carbon steel before and after exposure to industrial water alone and containing inhibitors were taken using SEM model JSM-5600 LV (JEOL Ltd.) interfaced with a computer and JSM software. The working potential was 20 kV and the specimen was kept under vacuum before taking images. The magnification range was x 500.

2. Results and Discussion

2.1 General

Values of corrosion current density (I_{cor}), corrosion potential (E_{cor}) and inhibition efficiency (IE) obtained from polarization measurements of low carbon steel at different temperatures and different concentrations of inhibitor in industrial water at 1.44 and 1.56 $m s^{-1}$ after 24 h of immersion time are depicted in **Table 1**. It is shown that, the Θ and IE increased with increasing the inhibitor concentration. From **Figures 2 and 5**, it is evident that the effect of velocity on the inhibition efficiency is more than that of the effect of temperature. The optimum concentrations of the studied plants found to perform the highest efficiency were 2.96 $g L^{-1}$ *Cucurbita pepo L* and 5.25 $g L^{-1}$ *Ocimum basilicum L*, with inhibition efficiency of 82.02% and 77.86% for *Cucurbita pepo* and *Ocimum basilicum* at 30 and 40°C, respectively at 1.56 $m s^{-1}$. Despite the presence of some oils and terpenes compounds in *Ocimum basilicum*, its IE is relatively less than that of *Cucurbita pepo*. This is because the *Cucurbita pepo* contains metal elements such as S, P, and K, and is also due to the presence of heterocyclic constituents like alkaloids and flavonoids which enhance the adsorption of the later on the low carbon steel surface. Further, the presence of potassium, K, aids in the metal surface being hydrophobic from its surface, thereby enhancing the adsorption on the metal surface to protect the metal for a long time. This consideration is enhanced by the higher negative values of ΔS_a for *Cucurbita pepo* which is -175.06 $J mol^{-1} K^{-1}$ at optimum conditions, whereas ΔS_a for *Ocimum basilicum L* is -174.60 $J mol^{-1} K^{-1}$ at optimum conditions.

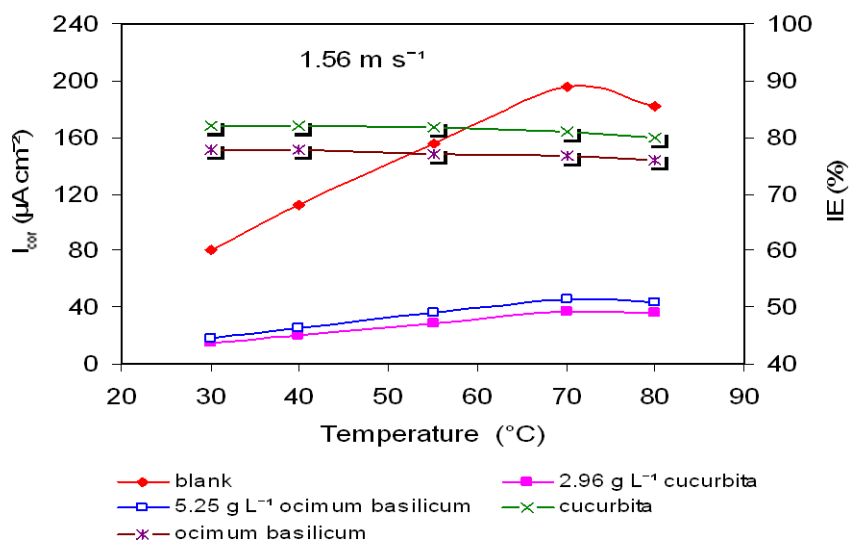


Fig.2 Effect of temperature on I_{cor} and IE in absence and at optimum concentration of *cucurbita pepo* and *Ocimum basilicum* at 1.56 $m s^{-1}$

Table 1 Electrochemical parameters obtained from polarization of low carbon steel in industrial water containing different concentrations of *Ocimum basilicum* and *Cucurbita pepo* at different temperatures and at 1.44 and 1.56 m s⁻¹

Plant	T [°C]	c [g L ⁻¹]	1.44 m s ⁻¹			1.56 m s ⁻¹		
			E _{cor} [mV vs. SCE]	I _{cor} [μA cm ⁻²]	IE _{Icor} [%]	E _{cor} [mV vs. SCE]	I _{cor} [μA cm ⁻²]	IE _{Icor} [%]
	30	blank	-500	62.50		-502	80.35	
		0.68	-494	38.66	38.15	-495	46.16	42.55
		1.00	-490	29.90	52.16	-489	36.57	54.49
		1.88	-480	23.82	61.89	-480	28.30	64.78
		2.15	-470	15.89	74.58	-472	20.22	74.83
		2.96	-464	11.39	81.78	-464	14.45	82.02
<i>Cucurbita pepo</i>	40	blank	-505	78.65		-508	112.3	
		0.68	-493	48.76	38.00	-496	64.93	42.18
		1.00	-492	37.67	52.11	-492	52.24	53.48
		1.88	-479	31.12	60.43	-480	41.05	63.45
		2.15	-474	20.85	73.49	-473	29.12	74.07
		2.96	-463	14.38	81.72	-465	20.19	82.02
<i>Ocimum basilicum</i>	30	blank	-500	62.50		-502	80.35	
		0.90	-498	51.13	18.19	-500	61.50	23.46
		1.78	-496	38.14	38.97	-496	46.93	41.59
		3.00	-490	27.82	55.49	-491	31.75	60.48
		4.12	-486	19.09	69.45	-479	22.38	72.15
		5.25	-480	14.86	76.23	-469	17.85	77.78
<i>Ocimum basilicum</i>	40	blank	-505	78.65		-508	112.3	
		0.90	-498	64.32	18.22	-500	87.41	22.16
		1.78	-496	47.64	39.43	-497	66.83	40.49
		3.00	-489	35.09	55.38	-493	45.23	59.72
		4.12	-486	23.50	70.12	-486	33.58	70.10
		5.25	-478	18.44	76.55	-470	24.86	77.86

2.2 Effect of temperature

Temperature is one of the main factors likely to modify the behavior of materials in a corrosive medium. Hence, the effects of various temperatures, ranging from 30 to 80°C, on the mechanism of corrosion rate in the absence and presence of different concentrations of the inhibitor have been investigated. From **Table 1** and **Figure 2**, it is shown that the I_{cor} sharply increases with increasing temperature in the absence of *cucurbita pepo* and *Ocimum basilicum*, except at 80°C. The decrease of I_{cor} at 80°C is attributed to the escape of oxygen from the open system, unlike in the close system. However, I_{cor} normally increases with increasing temperature in the presence of both plant extracts. However, the I_{cor} decreases with increasing concentration of the inhibitor. The relative decrease of IE at higher temperature of 1.56 m s⁻¹ suggests that since the rate of destruction of the adsorbed film is higher than its rate of formation, the adsorption process has a tendency to be a physisorption rather than chemisorptions, and the dissolution rate of low carbon steel takes place on an almost naked metal surface.

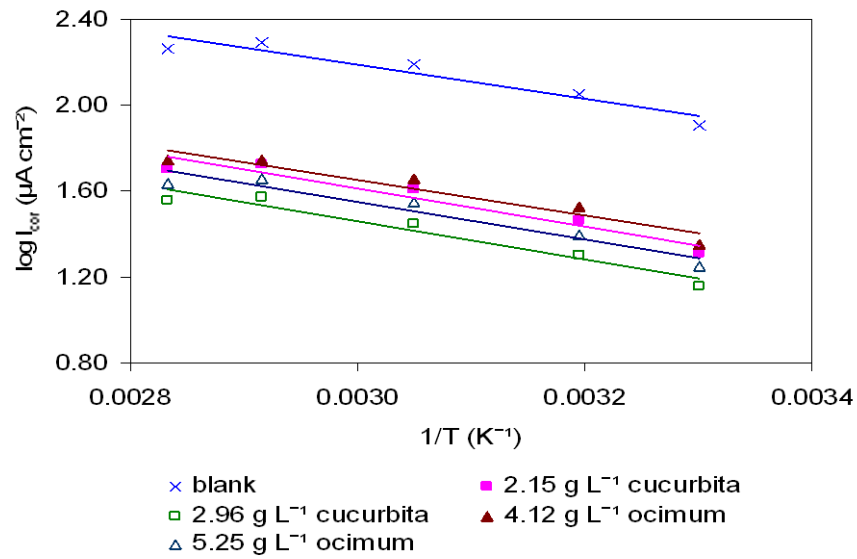


Fig. 3 Arrhenius plots for low carbon steel in industrial water in absence and presence of different concentrations of *Cucurbita pepo* and *Ocimum basilicum* at $1.56 m s^{-1}$

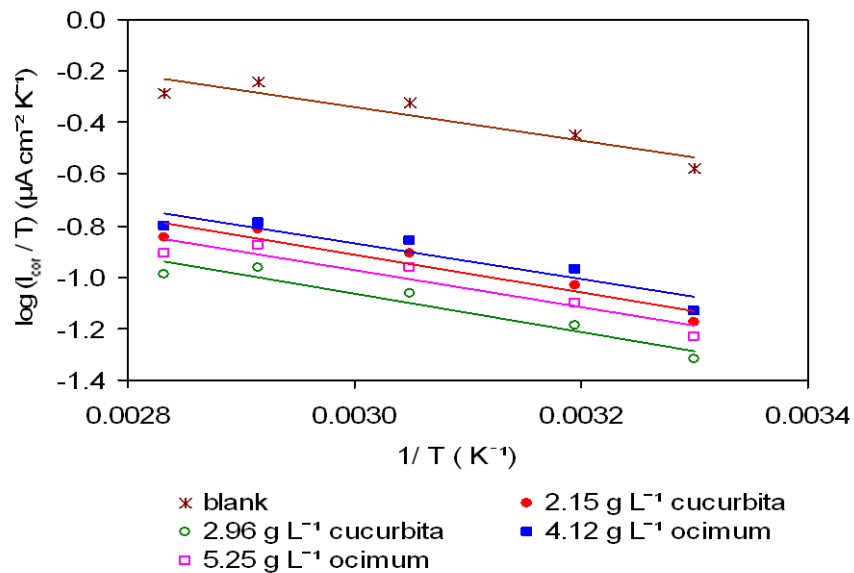


Fig. 4 Eyring plots for low carbon steel in industrial water in absence and presence of different concentrations of *Cucurbita pepo* and *Ocimum basilicum* at $1.56 m s^{-1}$

The activation energy for low carbon steel corrosion process was calculated using Arrhenius model by Eq. (5).

$$I_{\text{cor}} = k \cdot \exp\left(\frac{-E_a}{RT}\right) \quad (5)$$

The activation entropy (ΔS_a) and enthalpy (ΔH_a) were calculated from Eyring's equation as given by Eq. (6).

$$I_{\text{cor}} = \frac{RT}{hN} \exp\left(\frac{\Delta S_a}{R}\right) \cdot \exp\left(\frac{-\Delta H_a}{RT}\right) \quad (6)$$

where, E_a is the apparent activation energy, k is the pre-exponential factor, R is the universal gas constant, T is the absolute temperature, h is Plank's constant, N is Avogadro's number, and ΔH_a is the enthalpy. Plots of $\log I_{\text{cor}}$ and $\log (I_{\text{cor}}/T)$ versus $1/T$ give slopes of $(-E_a/2.303R)$ and $(-\Delta H_a/2.303R)$, as shown in **Figure 3** and **Figure 4**, respectively. The summarized values of the above parameters are given in **Table 2**. It is shown that, the values of E_a in the presence of *Cucurbita pepo* and *Ocimum basilicum* are higher than those of in its absence.

This indicates that the formation of the adsorptive film occurs by a physical mechanism on the metal surface [22]. The values of E_a increase with increasing concentration of inhibitors. This is attributed to the presence of plant extracts, which induce an energy barrier for the corrosion reaction that increases with increasing concentration of the inhibitor [23]. Typically, and according to Eq. (4), the higher value of E_a and the lower value of k lead to a reduction in the corrosion rate. In the present investigation, the results obtained are in agreement with that mathematical analysis stated. The positive values of ΔH_a reflect that the dissolution reaction is an endothermic process. The values of ΔS_a increased negatively in both the absence and presence of the inhibitors. This implies that the activation complex is the rate determining step that represents association rather than dissociation, indicating that a decrease in disorder takes place when going from reactants to the activated complex and isolated system [24]. Furthermore, the values of ΔH_a obtained are in good agreement with those obtained from Eq. (7).

$$\Delta H = E_a - RT \quad (7)$$

Table 2 Values of activation parameters k , E_a and ΔH_a for low carbon steel in industrial water in absence and presence of different concentrations of *Cucurbita pepo* and *Ocimum basilicum* at 1.56 m s^{-1}

Plant	c [g L ⁻¹]	k [μA cm ⁻²]	E_a [kJ mol ⁻¹]	ΔH_a [kJ mol ⁻¹]	$\Delta H_a = E_a - RT$ [kJ mol ⁻¹]
<i>Cucurbita pepo</i>	blank	36,957	15.20	12.49	12.68
	2.15	17,803	16.84	14.12	14.32
	2.96	13,378	17.01	14.30	14.49
<i>Ocimum basilicum</i>	4.12	14,240	15.96	13.25	13.45
	5.25	14,138	16.60	13.88	14.08

2.3 Effect of velocity

As the fluid flows through the pipe, the rotational speeds of the specimen were converted into flow rate of the fluid using the following empirical equations [25] of Eqs. (8) and (9).

$$q = 0.92nD_a^3 \left(\frac{D_t}{D_a}\right) \quad (8)$$

$$A_p = \pi D_a W_b \quad (9)$$

where, q is the total flow rate from the edges of the impeller [$\text{m}^3 \text{s}^{-1}$], n is the number of rotations per second, D_a is the impeller diameter [m], D_i is the diameter of solution vessel [m], A_p is taken as the area of the cylinder swept out by the tips of the impeller blades [m^2], and W_b is the width of the blades [m]. The velocity of the fluid can be obtained by dividing Eq. (8) by Eq. (9). [26] studied the corrosion rate of mild steel tubes with high purity water and observed that the rate increased with increasing speed of flow to a maximum value at about 3.3 ft s^{-1} (1.006 m s^{-1}). [27] reported that a maximum velocity 4 m s^{-1} is required to reduce fouling and the velocity of water are appropriate between 1.5 to 2.5 m s^{-1} .

Figure 5 shows that in the absence and presence of inhibitor, the corrosion current density (I_{cor}) increased with increasing velocity; and the inhibition efficiency (IE) was a maximum at 1.56 m s^{-1} . It is found that the velocity of 1.56 m s^{-1} is the appropriate velocity to distribute the inhibitors properly and keep the suspended particles from precipitating with the metal surface forming products, which results in pitting corrosion or erosion due to the flow along the surface. Beyond 1.56 m s^{-1} , the inhibition efficiency begins decreasing because the greater velocity, the thinner the laminar layer becomes along the metal surface [27], so oxygen easily reaches the metal surface and causes more corrosion. Moreover, at higher velocity, the extraneous impurities such as sand, dust and scales etc., embedded on the metal surface to cause pitting or scratching on the molecules of the adsorbed layer and removed the adsorbed film away from the metal surface.

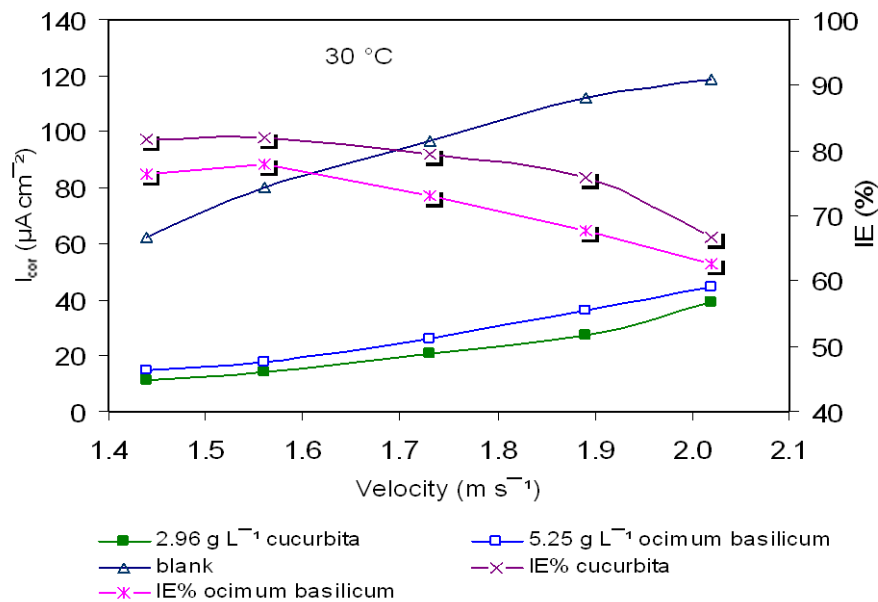


Fig. 5 Effect of fluid velocity on I_{cor} and IE in absence and at optimum concentration of *Cucurbita pepo* and *Ocimum basilicum* at 30°C .

2.4 Effect of immersion time

Figure 6 shows mass loss per unit area of low carbon steel versus immersion time and concentrations of *cucurbita pepo* at 1.56 m s^{-1} and 30°C . It is shown clearly that the mass loss per unit area in the uninhibited solution increases with increasing immersion time due to the anodic and cathodic dissolution. It is evident that the mass loss per unit area in the presence of the inhibitors was nearly independent of immersion time ($dy_{\text{cor}}(t)/dt \approx 0$). The linear variation of mass loss per unit area with time in plain and inhibited solution shows the absence of insoluble product on low the carbon steel surface.

The relatively large divergence of the plots between absence and presence of inhibitors indicates the increase of IE with concentration and to retain it constant with time. This is attributed to the fact that the film forms at the surface, which limits the dissolution of the latter by blocking its corrosion sites. This may be correlated with the progressive formation for inhibitor molecules as a protective film on the metal surface. Therefore, the

electrolyte hardly penetrates the porous layers to attack the metal surface. Moreover, at the same time, the increase of inhibitor concentration above a certain value has little effect on the inhibition efficiency. On the other hand, above 2.96 and 5.25 g L⁻¹ of *Cucurbita pepo* and *Ocimum basilicum*, the influence of concentration is very insignificant and can be ignored.

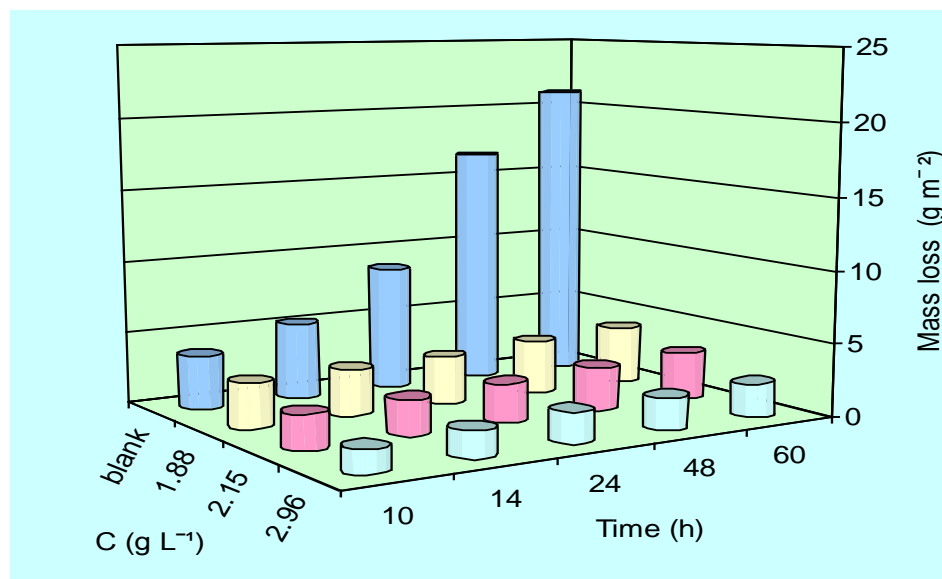


Fig. 6 Effect of immersion time on mass loss for low carbon steel in absence and presence of *Cucurbita* in industrial water at 30°C and at 1.56 m s⁻¹

2.5 Potentiodynamic polarization

Effects of addition of *Cucurbita pepo* and *Ocimum basilicum* on the anodic and cathodic polarization curves of low carbon steel in industrial water at various temperatures and at various velocities have been studied. The effects of increased concentration of *Cucurbita* and *ocimum* on the anodic and cathodic curves and on the Tafel slopes are represented in **Figures 7(a) and (b)**, respectively. The corrosion current density (I_{cor}) and corrosion potential (E_{cor}) are determined from the intersection of the extrapolating anodic and cathodic Tafel lines and are given in **Table 1**. Surface coverage degree (θ) and inhibition efficiency (IE) are calculated and given in Table 1. Inspection of Table 1 and Figures 10a and 10b reveals that increasing in the concentrations of the additive shows the following:

(1) The Tafel lines are shifted to more positive and negative potential for anodic and cathodic processes, respectively, relative to the blank curve. This means that these compounds influence both cathodic and anodic processes. However, the data suggest that these compounds act mainly as anodic inhibitors, where the anodic is more polarized when an external current is applied (anodic slope > cathodic slope), because the presence of terpenes and flavomoids in the studied plant extracts may act as acids in the neutralization medium.

(2) E_{cor} is shifted to more positive, and the values of I_{cor} decreased indicating the inhibiting effect of these compounds. These behaviors suggest that the extracts inhibit the corrosion of low carbon steel via adsorption of their molecules on both anodic and cathodic sites; however, Tafel slopes towards the anode were larger than the cathode and, consequently, the compounds predominate as anodic inhibitors for low carbon steel.

(3) Inhibition efficiency is improved by increasing the inhibitors concentration. This is attributed to the fact that oxygen in air easily permeates the thin solution layer to the metal surface. The corrosion reaction of low carbon steel occurs in the thin electrolyte layer; however, in the presence of the studied inhibitors, the compounds can bond into a stable protective layer on the metal surface. As a result of this, the anodic dissolution of low carbon steel has been obstructed by the protective layer.

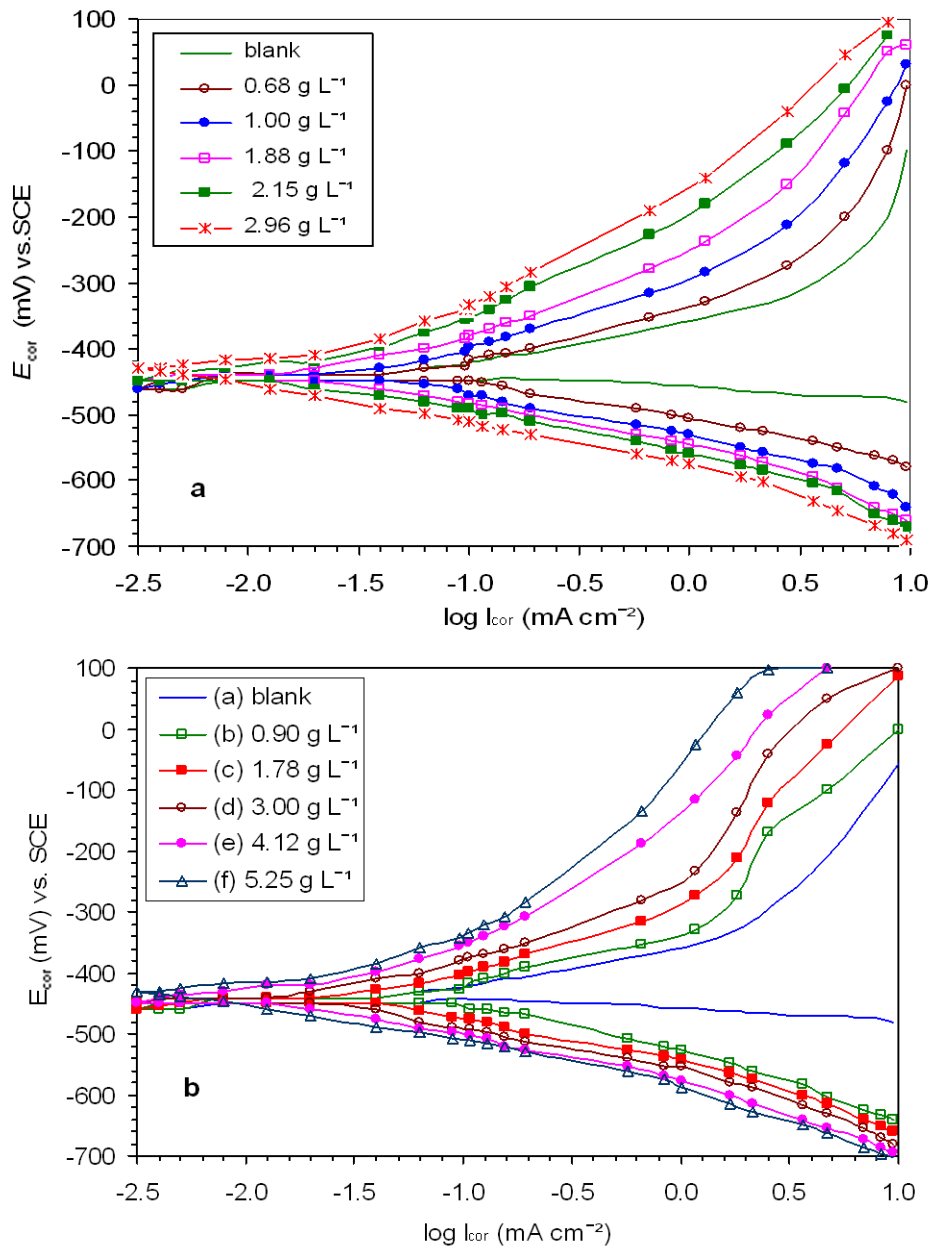


Fig.7 Potentiodynamic polarization curves of low carbon steel in industrial water in absence and presence of different concentrations of (a) *Cucurbita* and (b) *Ocimum* at 30°C and at 1.56 m s⁻¹

2.6 EIS studies

The corrosion behavior of low carbon steel in industrial water solution in the presence and absence of plant extract has been investigated by EIS at 30°C and at 1.56 m s⁻¹ after an exposure period of 30 min. The impedance (Z) depends on the charge transfer resistance (R_{ct}), the solution resistance (R_s), the capacitance of the electrical double layer (C_{dl}), and the frequency of the AC signal (ω). R_{ct} represents the difference of the diameter at high and low frequency on the peak-value-phenomenon. Therefore, C_{dl} can be obtained from Eq. (17).

$$C_{dl} = \frac{1}{2\pi f_{max} R_{ct}} \quad (17)$$

where, f_{max} is the maximum frequency

$$Z = Z' + jZ'' = R_s + \frac{R_{ct} + j(R_{ct}^2 C_{dl} \omega)}{1 + (R_{ct} C_{dl} \omega)^2} \quad (18)$$

The high-frequency intercept is equal to the solution resistance, and the low-frequency intercept is equal to the sum of the solution and charge transfer resistance. **Figures 8(a) and (b)** show the Nyquist plots of *Cucurbita pepo* and *Ocimum basilicum* at different concentrations. The magnitude of the impedance increased continuously from blank to 2.96 g L⁻¹ and 5.25 g L⁻¹ for *Cucurbita* and *ocimum*, respectively which is in accordance with the results in **Figures 8 (a) and (b)**.

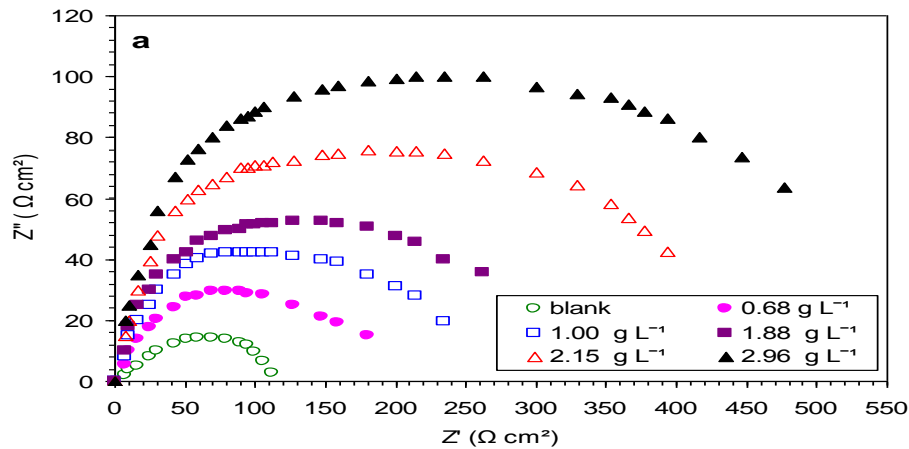


Fig.8 Nyquist plots for low carbon steel in industrial water in the absence and presence of different concentrations of (a) *Cucurbita* and at 30°C and at 1.56 m s⁻¹

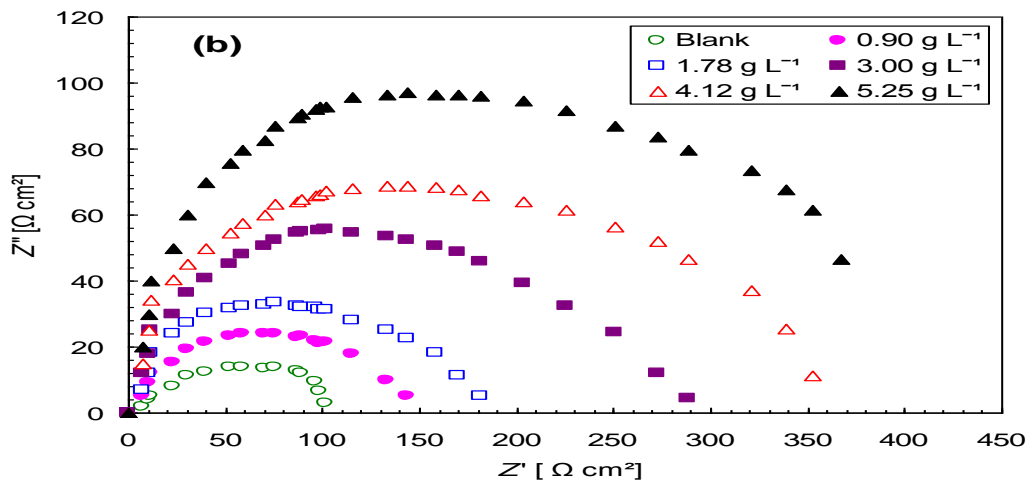


Fig.8 Nyquist plots for low carbon steel in industrial water in the absence and presence of different concentrations of (b) *Ocimum* at 30°C and at 1.56 m s⁻¹

The impedance diagram obtained with free industrial (without inhibitors) water shows only one capacitive loop. The same trend (one capacitive loop) is also noticed for low carbon steel immersed in industrial water containing plant extract (0.68 – 2.96) g L⁻¹ for *Cucurbita* and (0.90 – 5.25) g L⁻¹ for *ocimum*. The diameter of Nyquist plots increases with increasing the plant extract concentrations. This suggests that the formed

inhibitive film is strengthened by the addition of plant extracts. The main parameters deduced such charge transfer resistance (R_{ct}) and double layer capacitance (C_{dl}), from the analysis of the Nyquist diagram for low carbon steel in industrial water medium containing various concentrations of plant extract are given in **Table 3**. R_{ct} and C_{dl} have opposite trends at the whole concentration range. R_{ct} gradually increases with the increase of inhibitor concentration up to 2.96 (critical values) and 5.25 g L⁻¹ for *Cucurbita* and *ocimum*, respectively. A further increase of inhibitor concentration has no effect on R_{ct} . However, double layer capacitance C_{dl} decreases continuously with the increase of inhibitor concentration up to 2.96 and 5.25 g L⁻¹. Hence, both R_{ct} and C_{dl} showed the peak value-phenomenon (lowest corrosion rate) at critical values of inhibitors concentration. This could be associated with adsorption mode of the inhibitor [33, 34]. The impedance data show that the inhibition of *Cucurbita* and *Ocimum* is characterized by an increase in the diameter of capacitive arc that acts as the resistance. In other words, the impedance complex plane plots are similar to a depressed semicircle approaching a capacitor, which indicates that a homogenous protective layer is formed on the metal surface, and the corrosion process has become more difficult in the presence of the investigated compounds [35]. When inhibitor concentration is lower than the critical values, adsorbed inhibitor molecules are parallel to the metal surface and decrease the number of surface active sites. The higher the inhibitor concentration is the more inhibitor molecules are adsorbed on the metal surface and the surface active sites are blocked. Also, it can be observed that $IE_{R_{ct}}$ are in good agreement with those obtained in the case of potentiodynamic.

Table 3 Impedance parameters and the corresponding inhibition efficiency for low carbon steel in industrial water in the absence and presence of radish leaves and black cumin at 30°C and 1.56 m s⁻¹

Inhibitors	Concentration [g L ⁻¹]	R_{ct} [Ω cm ²]	C_{dl} [μ F cm ⁻²]	$IE_{R_{ct}}$ [%]
	blank	98.00	151.67	–
<i>Cucurbita pepo</i>	0.68	165.51	46.49	40.79
	1.00	224.36	31.72	56.32
	1.88	271.24	20.28	63.87
	2.15	423.69	12.37	76.81
	2.96	520.98	2.02	81.19
<i>Ocimum basilicum</i>	0.90	131.33	97.48	25.38
	1.78	179.09	39.17	45.28
	3.00	270.05	21.85	63.71
	4.12	360.82	17.31	72.84
	5.25	409.87	12.66	76.09

2.7 SEM analyses

SEM analyses are conducted in order to characterize the protective layer that formed on the low carbon steel surface. SEM images of polished low carbon steel and low carbon steel in uninhibited and inhibited solutions at 30°C and at 1.56 m s⁻¹ are presented in **Figures 9 (a) to (d)**, respectively. After exposure of low carbon steel to uninhibited solution, the corroded surface appeared to dissolve uniformly with large valleys and deep terraces (**Figure 9(b)**). In the presence of optimum concentration of *Cucurbita* and *Ocimum* extracts, the corroded surface shows small and very smooth valleys or grooves as shown in **Figures 9(c)** and **(d)** respectively. However, the surface in the presence of *Cucurbita* (**Figure 9(d)**) is smoother than that in the presence of *Ocimum* (**Figure 9 c**). This is attributed to the complex film of Fe-plant extracts formed on the surface, thereby offering better protection towards low carbon steel corrosion. This shows that this plant extract inhibits corrosion of low carbon steel in industrial water solution. After 10 h of immersion in the inhibited solution, the low carbon surface is partly covered with a layer containing the molecules of plant

extracts. It can be concluded from this analysis that the molecules of plant extracts are incorporated in the surface of low carbon steel either as precipitate or, more likely, as part of the protective layer.

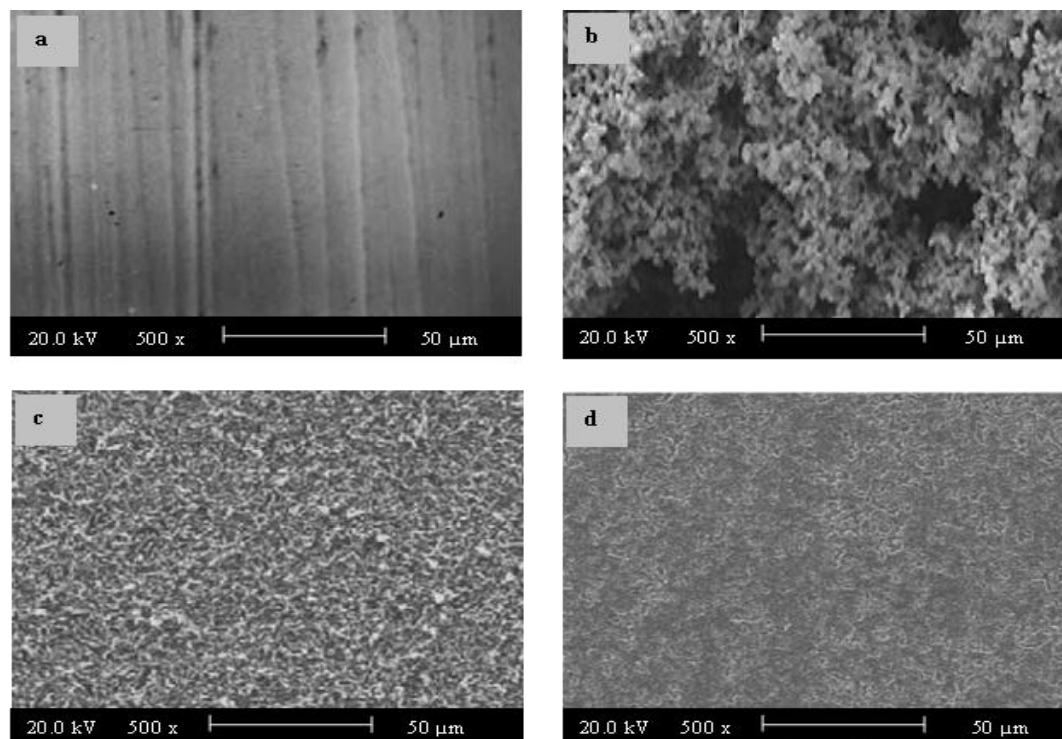


Fig. 9 SEM micrographs of low carbon steel (LCS): (a) free polished LCS; (b) LCS after immersion in uninhibited industrial water; (c) LCS treated by 5.25 g L^{-1} *Ocimum bacilicum*; and (d) LCS treated by 2.96 g L^{-1} *Cucurbita pepo*

Conclusion

The adsorption of *Cucurbita pepo* and *Ocimum bacilicum* is found to obey Flory-Huggins adsorption isotherm, and the inhibition efficiency was independent of temperature. The effect of velocity on the inhibition efficiency is more than the effect of temperature. The adsorbed film containing the investigated compound is identified by SEM images to reveal a good protective film on the metal surface in the presence of inhibitors. Polarization curves indicated that the *Cucurbita* and *Ocimum* act as anodic inhibitors for low carbon steel in industrial water. The inhibitive performance was improved by increasing the concentration of *Cucurbita* and *ocimum*, and by setting the velocity and temperature at optimum conditions. The inhibitive effect of *Cucurbita pepo* was better than that of *Ocimum bacilicum*. The thermodynamic parameters reveal that the inhibition of corrosion by these plants extract is due to the formation of a physisorption film on the metal surface. The weight loss (values not mentioned), potentiodynamic polarization and impedance are in reasonable good agreement. The charge transfer resistance was higher at the peak-value-phenomenon, whereas the double layer was lower showing the good inhibition and optimum concentration of the inhibitors were the critical at that point.

Acknowledgment

One of the authors is grateful to Mr. Nasr Humaidy for his help. This work was supported from Higher Education and Scientific Research, Yemen. As well as many thanks to Mysore University lab.

References

1. Abd-El-Rehim S.S., Refaey S. A. M., Taha F., Saleh M. B. and Ahmed R. A., *J. Appl. Electrochem.*, 31 (2001) 429- 435.
2. Abdullah, M. E. A., Helal and Fouda, A. S., *Corros. Sci.*, 48 (2006) 1639-1654.
3. Ananda, R. L. S., Maruthamuthu, S., Selvanayagam, M., Mohanan, S. and Palaniswamy , *Indian. J. Chem. Technol.* 12 (2005) 356-360.
4. Bastida, J. M., Dedamborenea, J. and Vazquez, A. J., *J. Appl. Electrochem.*, 27 (1997) 345-349.
5. Boffardi, B. P., and Schweitzer, G.W., "Water Quality, Corrosion Control and Monitoring, 9th International Congress on Metallic Corrosion", Toronto, Canada, 1984, p.404.
6. Bouklah, M., Benchat, N., Hammouti, B., Aouniti, A. and Kertit, S., *Mater. Lett.*, 60 (2006) 1901-1905.
7. Butler, G., and Stroud, E. G., *J. Appl. Chem.*, 15 (1965) 325-338.
8. Chetouani, A., and Hammouti, B., *Bull. Electrochem.*, 19 (2003) 23-25.
9. Chiej, R.; Encyclopaedia of Medicinal Plants, MacDonald, Edinburgh, U.K. 1984 , pp 255-264.
10. Dedamborenea, J., Bastida, J. M. and Vazquez, ? *Electrochim. Acta*, 42 (1997) 455- 459.
11. Donahue, F. M., and Nobe, K., *J. Electrochem. Soc.*, 112 (1965) 886-891.
12. El-Etre, A. Y., *Corros. Sci.*, 40 (1998) 1845- 1850.
13. El-Etre, A. Y., and Abdallah, M., *Corros. Sci.*, 42 (2000) 731-738.
14. Facciola, S., "Cornucopia - A Source Book of Edible Plants, Kampong Publications", U.K. 1990.
15. Fiala, A., Chibani, A., Darchen, A., Boulkamh, A. and Djebbar, K., *App. Sur. Sci.*, 253 (2007) 9347-9356.
16. Flory, P. J., *J. Chem. Phys.*, 10 (1942) 51-61.
17. Gao, G., Hao Liang, C. and Wang, H., *Corros. Sci.*, 49 (2007) 1833-1846.
18. Hammouti, B., Kertit ,S. and Mellhaoui ,M., *Bull. Electrochem.*, 11 (1995) 553-560.
19. Horvath, T., and Kutson, E., *Gyogy, Adam, Magy. Kem. Foly.* 98 (1997) 363-369.
20. Khamis, E., Bellucci, F., Latanision, R. M. and El-Ashry, E. S. H., *Corrosion*, 47 (1991) 677-681.
21. Khamis, E., and Al-Andis, N., *Materialwiss. Werkstofftech*, 33 (2002) 550-554.
22. Lopez, D. A., Simison, S. N. and de Sanchez, S. R., *Corros. Sci.*, 47 (2005) 735-755.
23. Minhaj, A. P. A., Quarishi , M. A. and Farooqi, I. H., *Corros. Prev. Control*, 46 (1999) 32-38.
24. Moutarlier, V., Gigandit, M. P., Normand, B. and Pagetti, J., *Corros. Sci.*, 47 (2005) 937-951.
25. Noor, E. A., *Corros. Sci.*, 47 (2005) 33-55.
26. Parikh, K. S., and Joshi, K. J., *Trans. SAEST* , 39, 64-68 (2004) Putilova, I. N., S. A. Balezin and V. P. Barannik, *Metallic Corrosion Inhibitors,*" *J. Electrochem. Soc.*, 108 (1961) 234-255.
27. Raja, P. B., and Sethuraman, M. G., *Mater. Lett.*, 62 (2008) 113-116.
28. Roberston, W., *J. Electrochem. Soc.*, 98 (1951) 94-100.
29. Saleh, R. M., Ismail, A. A. and El-Hosary ,A. A., *Br. Corros. J.*, 17 (1980) 131-135.
30. Sinnott, R. K., "Chemical Engineering Series", Vol. 1, 1st ed., Pergamon Press, Oxford, U.K. 1983.
31. Srivatsava, B. C., and Sanyal, B., "Cathodic Protection for Pipelines, Proc. Symposium of Cathodic Protection", Kanpur, India, 1973a, p. 52.
32. Srivatsava, K., and Sanyal, B., "Cathodic Impressed Current Protection, Proc. Symposium of Cathodic Protection", Kanpur, India, 1973b, p.19.
33. Srivatsava, K., and Srivatsava, P., *Br. Corros. J.*, 16 (1981) 221-227.
34. Wang, H. L., Fan, H. B. and Zheng, J. S., *Mater. Chem. Phys.*, 77 (2002) 655-661.
35. Waren, L. , Julian, C. S. and Hariott, P., "Unit Operations of Chemical Engineering", 4th ed, McGraw Hill, New York, U.S.A, 2003.

(2013); <http://www.jmaterenvirosci.com>